A novel low-temperature growth and characterization of single crystal ZnO nanorods

Chin-Hsien Hung, Wha-Tzong Whang*

Department of Materials Science & Engineering, National Chiao Tung University, 1001 Ta Hsueh Road, Hsin Chu, Taiwan 300, PR China

Abstract

One-dimensional (1D) single crystal ZnO nanorods directly grown on ZnO nanostructured substrates by soft chemical method is proposed. Employing a novel two steps procedure, the ZnO nanorods with a diameter about 45 nm can be successfully grown on substrate in aqueous solution at attractive low temperature in 90 °C, permitting large-scale fabrication with a relatively low cost and a potential application in optoelectronic nanodevices. The structures, appearances and optical properties of ZnO nanorods also have been characterized.
© 2003 Elsevier B.V. All rights reserved.

Keywords: Zinc oxide; Nanorods

1. Introduction

Recently, one-dimensional (1D) nanoscale materials have received considerable attention due to their remarkable properties applied in optoelectronic and electronic nanodevices [1,2]. Particularly, semiconductor nanomaterials, such as GaN [3], CdS [4], Si [5] and MnO_2 [6], have been highly interested for the fundamental concepts of quantum size effect on optical, electrical and mechanical properties. Among them, ZnO notably possesses the unique properties such as wide direct-band gap (3.4 eV) and large exciton binding energy (60 meV) at room temperature, leading to a wide variety of potential applications in catalysts, gas sensors, piezoelectric devices, and solar cells [7,8]. Moreover, ZnO nanowire array is shown to have a UV-laser emission in the room temperature, as has been observed by Yang and co-workers [9]. Generally, 1D ZnO nanowhisker can be prepared by various methods, including using anodic alumina template [10], vapor–liquid–solid (VLS) mechanism [11], metal-organic vapor-phase epitaxial growth (MOVPE) [12,13] and common thermal evaporation method [14–17]. However, all the above methods always require quite extreme conditions and expensive equipments. Contrariwise, the soft chemical process provides a mild condition with a low-cost and well-controlled method to synthesize 1D nanoscale materials. Until now, the most effective ways

to fabricate 1D ZnO nanostructures by employing soft solution process are micro-emulsions growth [18], thermal decomposition reaction in solvent [19] and spray pyrolysis [20]. Although the soft chemical method can be used to grow 1D ZnO nanomaterials, however, most ZnO nanorods are randomly grown in the solutions, which limit their applications in nanodevices. Recently, ZnO microrod arrays have been be produced by using soft chemical method [21], however, the preparation of small diameter nanorods (diameter <100 nm) with controlled nano-size nucleation are still highly required. Herein, we demonstrate an effective technique to directly grow single crystal ZnO nanorods on substrates with high density. Notably, we employ ZnO nanostructured (ZnO nanoparticles/ITO) substrates, as self-seeding to control ZnO nanorod growth, which not only has an attractive low-temperature (ca. 90 °C) feature but also prevents from using exotic metal as catalysts. The exclusion of exotic metal catalyst is very important for fabricating reliable nanodevices based on high quality 1D nanorods, because even very low impurity concentration of catalyst could dopant species into semiconductor nanorods and significantly affect the properties of nanodevices. In this study, the ZnO nanostructured substrate is shown to be helpful to the ZnO nanorods formation by soft solution method, and a novel two-step procedure is proposed. In the first step, uniform ZnO nanoparticle colloids were synthesized by sol–gel reaction. Second, ITO glass substrates covered with ZnO nanoparticle seeds were used to grow the nanorods from the hydrolysis–condensation of Zn^{2+} salt

* Corresponding author. Tel.: +886-3-571-2121; fax: +886-3-572-4727.
E-mail address: wtwhang@msn.com (W.-T. Whang).
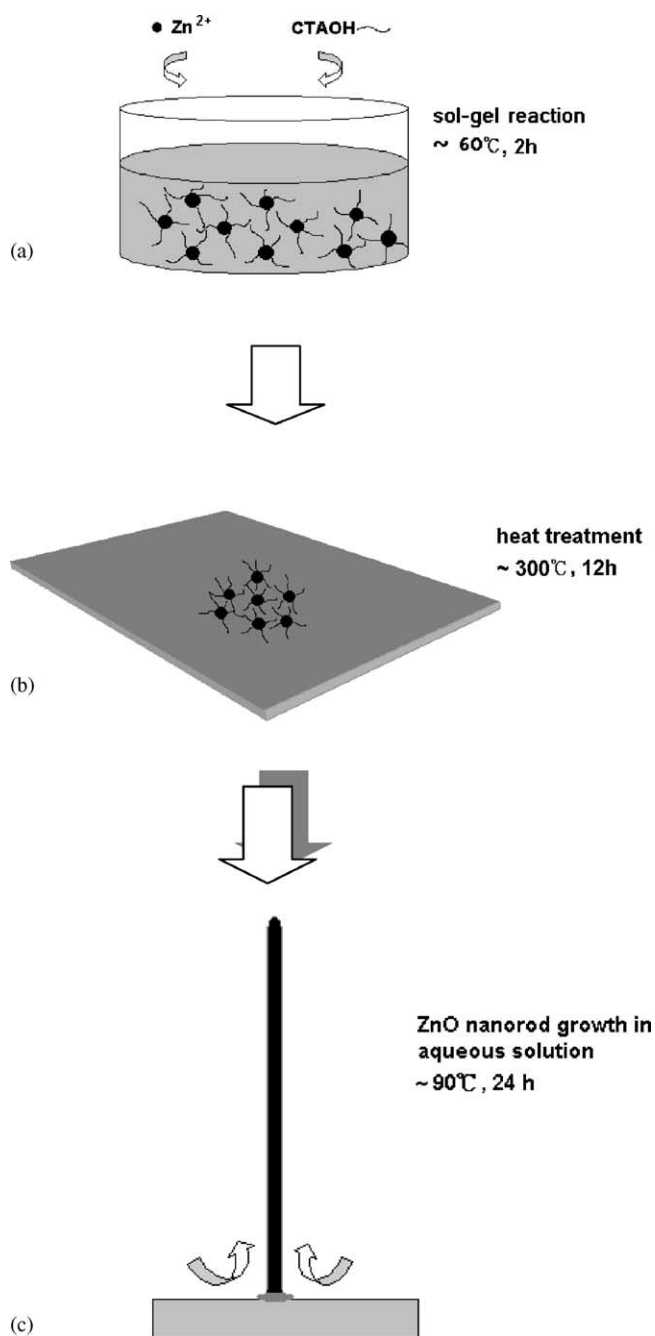
(a)

(b)

(c)

Fig. 1. A schematic illustration for ZnO nanorod growth on nanostructured substrate by soft chemical method: (a–b) formation of ZnO nanoparticle colloids through sol–gel reaction and dispersion on ITO substrate; (c) the ZnO nanorods directly grow from the nanoparticles via hydrolysis–condensation process.

aqueous solution. The schematic diagram illustrating the ZnO nanorods formation processes is shown in Fig. 1.

2. Experimental procedure

All the chemicals from Tokyo Chemical Industry were used as received without further purification.

2.1. Preparation of ∼4.3 nm ZnO nanoparticle seeds

The ZnO nanoparticles were prepared by sol–gel reaction with cetyltrimethylammonium hydroxide (CTAOH) as both catalysts, and surfactants (Fig. 1(a)). The 0.01 M of zinc acetate [$Zn(CH_3COOH)_2 \cdot 2H_2O$] was dissolved in ethanol under vigorous stirring at 60 °C for 1 h, then cooled to 0 °C. The cetyltrimethylammonium hydroxide was then added into the solution with a molar ratio of Zn^{2+}/CTAOH = 1/1.6 under constant stirring for 30 min. The mixture was subsequently refluxed at 60 °C for 2 h to grow ZnO nanoparticles and allowed cooling to room temperature.

2.2. Growth of ZnO nanorods

The ZnO nanoparticle colloids were directly dipped into ITO substrates and dried at room temperature. Before growing nanorods, the nanostructured substrate was under the heat treatment in dry air at 300 °C for 12 h (Fig. 1(b)). Then ZnO nanostructured substrates were immersed in equimolar of zinc nitrate ($Zn(NO)_3 \cdot 6H_2O$) and methenamine ($C_6H_{12}N_4$) aqueous solutions at 90 °C for 24 h to grow ZnO nanorods (Fig. 1(c)). Finally, the grown ZnO nanorods on nanostructured substrates was thoroughly washed with deionized water and allowed drying in air at room temperature.

The ZnO nanorods were further characterized and analyzed by scanning electron microscopy (SEM, Hitachi S-4700 FEG at 15 kV), Transmission electron microscopy (TEM, JOEL 2000FX at 200 kV), Philip Tecnai 20 high-resolution TEM (HRTEM) at 200 kV equipped with a GATAN digital photograph system and energy dispersion X-ray spectroscopy (EDS). The absorption spectrum was recorded by a HP8453 UV-Vis spectrometer. The Raman spectra were measured by Renishaw system 2000 micro-Raman spectrometer with a 514 Ar^+ laser as excitation source. Photoluminescence (PL) spectra were also performed at room temperature using a He:Cd laser with a wavelength of 325 nm. An X-ray diffraction study of the samples was carried out with MAC Sience MXP18 X-ray diffractometer (30 kV, 20 mA) with copper targets at a scanning rate of $4°\,min^{-1}$.

3. Result and discussion

3.1. Characterization of the ZnO nanoparticles

The UV-Vis absorbance spectrum of the ZnO nanoparticle colloids is shown in Fig. 2. The absorption spectrum shows a well-defined exciton band at 327 nm and significant blue shift relative to the bulk exciton absorption (373 nm) [22]. This shift phenomenon mainly corresponds to the confinement effect of the small size ZnO nanoparticle colloids (particle size ≤7 nm) [23]. According to the experimental relationship between the absorption shoulder ($\lambda_{1/2}$) and the
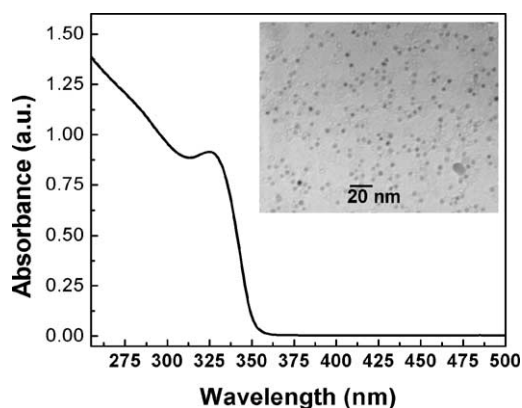
Fig. 2. Absorption spectrum and TEM image (inset) of CATOH-capped ZnO nanoparticles.

particle size reported by Meulenkamp [24], the diameter difference of the nanopartices during aging at 60 °C can be monitored. After aging for 2 h, the particles average diameter is estimated to ~3.6 nm, which consists with our TEM measurement. In the TEM image (shown in inset of Fig. 2), the nanoparticles are essentially monodispersed. Moreover, the nanoparticles are almost fully well separated, indicating that CTAOH surfactants efficiently cap on the particle surfaces and successfully prevent the aggregation from sol–gel reaction.

3.2. Characterization of the as-grown ZnO nanorods

Fig. 3 shows the typical field emission SEM images of ZnO nanorods grown on nanostructured substrate at 90 °C aqueous solution. The SEM images clearly show that straight nanorods can be grown on the whole substrate surfaces with high density. Although the nanorods are not perfectly aligned on the substrate, they have a tendency to grow perpendicularly above the surfaces. The nanorods grown with 10×10^{-3}, 8.4×10^{-3} and 6.8×10^{-3} M Zn^{2+} aqueous solutions at 90 °C for 24 h exhibit mean diameters of about 50, 45 and 40 nm, respectively (Figs. 3(a)–(c)). The diameters of nanorods grown at higher concentration (17×10^{-3} and 20×10^{-3} M) increase to about 100 nm, implying that nanorods diameters strongly depend on the concentration of aqueous solution. Meanwhile, as shown in the inset of Fig. 3(a), the ZnO nanorod has a hexagonal prismatic cross-section and a hemispherical end. For identifying the growing sites of the nanorods on the nanostructured substrates, pure ITO substrates without ZnO nanoparticles were used with the same experimental conditions. However, quite barely nanorods are grown on the pure substrates indicating that ZnO nanoparticles obviously play a crucial role in the ZnO nanorod growth processes.

The crystal structure of as-grown ZnO nanorods was investigated using XRD (Fig. 4(a)). The [0 0 2] reflection apparently has sharpened up compared with the [1 0 1] maximum reflection of ZnO zincite (JCPDS 36-1451), indicating that the ZnO nanorods are grown with c-axis
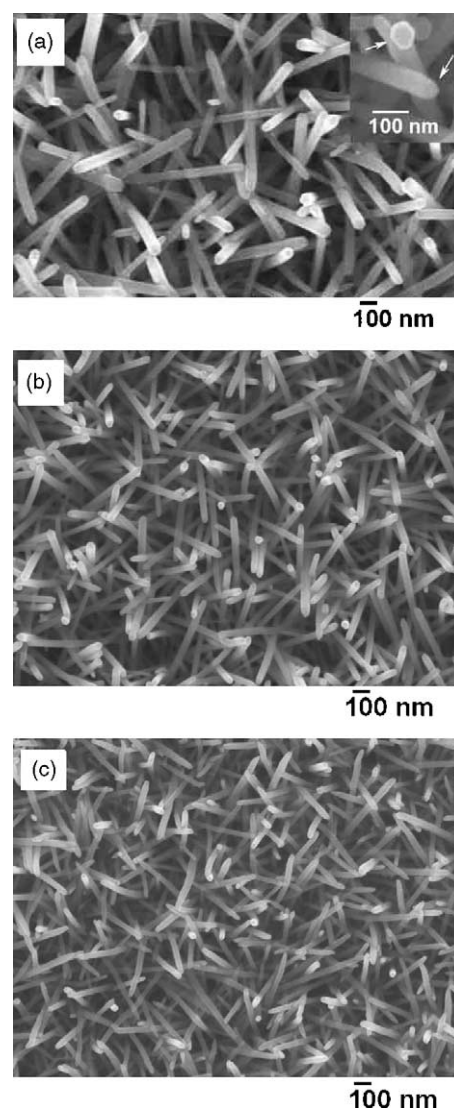

Fig. 3. SEM image of ZnO nanorods grown in aqueous solution on the nanostructured substrate. The corresponding concentration of Zn^{2+} aqueous solution is (a) 10×10^{-3}, (b) 8.4×10^{-3} and (c) 6.8×10^{-3} M. The inset in Fig. 3(a) exhibits hexagonal prismatic cross-section and a hemispherical end.

orientation and trend perpendicular to the substrate surface. Fig. 4(b) shows Raman spectra of ITO substrates and ZnO nanorods grown on the substrates. Clearly, the ZnO nanorods have only one peak at $432 \, cm^{-1}$ corresponding to ZnO optical phonons E_2 mode [25].

In order to characterize the ZnO nanorods, TEM was employed to observe the nanorod microstructure. To prepare TEM samples, the nanorods were scraped from substrate by brief ultrasonication in methanol, and then dispersed onto a carbon film covered copper grid. In Fig. 5(a), the bright-field TEM image of nanorods shows that the typical diameters and length-to-diameter ratios are about 50 and 25 nm, respectively. Notably, individual nanorod has one hemispherical end and another flat end in Fig. 5(a). Compared with Fig. 3(a), we suggest that the nanorods could be grown
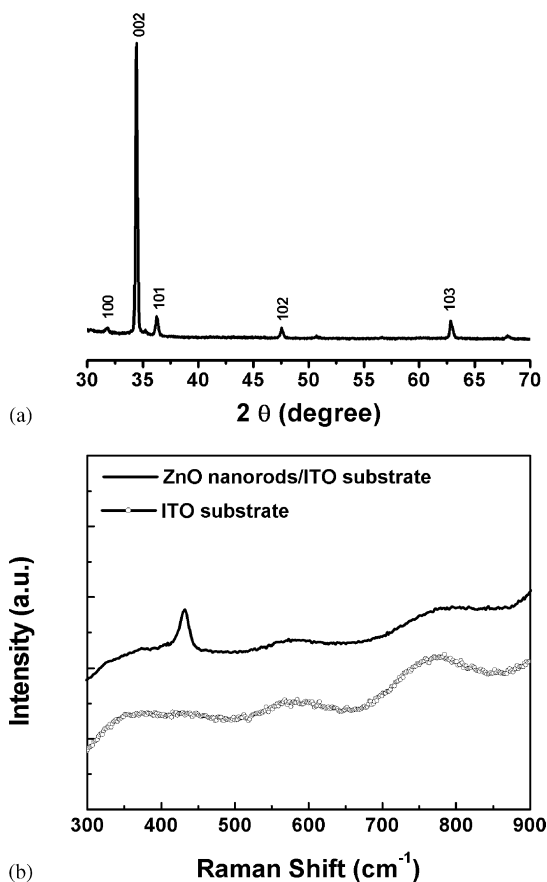
Fig. 4. (a) The XRD pattern and (b) Raman spectrum of the ZnO nanorods on ITO substrate.

Fig. 5. (a) TEM and select area diffraction image of single crystal ZnO nanorods grown in 10×10^{-3} M Zn^{2+} aqueous solution. The diffraction pattern shows that the nanorod grows along [0 0 0 1] direction. (b, inset) High resolution TEM image obtained from the edge of an individual nanorod and its corresponding SAED pattern. The incident beam is along the zone axis.

from the well-defined faceted end to the hemispherical end, which is similar to the previous reports on the single crystal ZnO whiskers [26,18]. In addition, the EDS analysis of nanorods showed only contain Zn and O, indicating that there is no other metal impurity as catalysts. The HRTEM lattice fringes image and selected area electron diffraction (SAED) pattern shown in Fig. 5(b) reveal that, in this region, the nanorods possess a single crystal hexagonal structure without dislocations and stacking faults. The image also confirms that the nanorods grow along the [0 0 0 1] direction (indicated with an arrow).

Photoluminescence (PL) of the ZnO nanorods were measured in room temperature and the spectra were shown in Fig. 6. In Fig. 6(a), a sharp near band-edge emission at 378 nm and a broad green emission at ∼580 nm can be observed. The near band-edge emission is attributed to a well-known recombination of free excitons [27], and the green emission is resulted from the recombination of photo-generated hole with a singly ionized charge state of specific defect [28]. In addition, the heat-treatment step further decreases green emission intensity and increases band-edge emission intensity (Fig. 6(b)). This result can be attributed to that decrease in the amount of the singly ionized oxygen vacancies in the ZnO, so high crystal
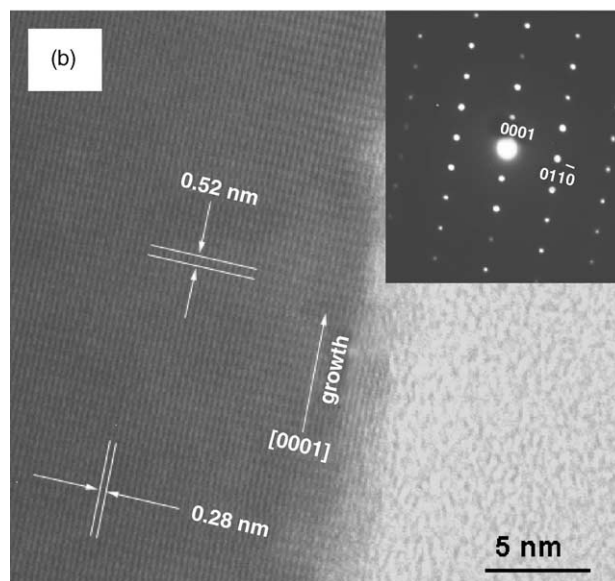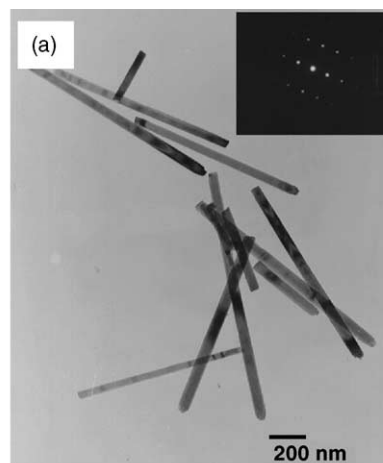
quality of ZnO nanorods can be produced via high temperature heat-treatment processes.

In order to realize the influence of nanoparticles on the nucleation and growth of ZnO nanorods, more detailed experiments were carried out. First, the effects of various concentrations of the nanoparticles precursor were investigated. Experiment results show that the precursor concentration increases to ∼0.05 M, the average nanorods diameters and lengths increase to 70 ± 25 nm and ∼3 μm (Fig. 7(a)). The diameter increasing could be attributed to the seeds aggregation, because high concentration precursors form bigger nanoclusters and large size seeds, subsequently tend to the growth of coarser nanorods. Fig. 7(b) is the TEM image of such nanorods, showing that nanorods are straight along the longitudinal axis. Second, the lower
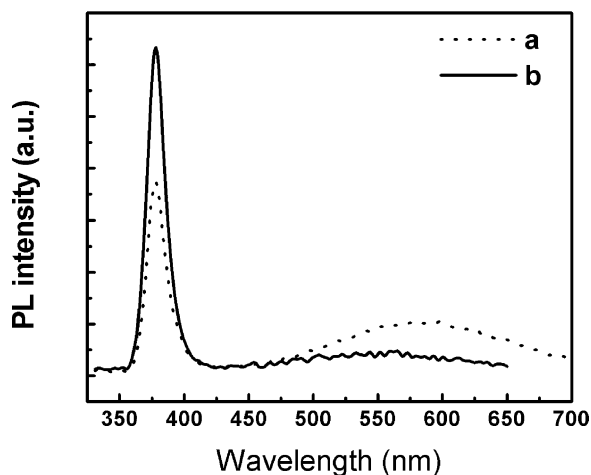
Fig. 6. PL spectra of: (a) before and (b) after heating at 350 °C for 12 h.

Fig. 8. SEM image of the ZnO nanorods grown at the same condition but using the nanostructured substrate with low-heat treatment temperature of ~250 °C.

heat-treatment temperature for preparing the nanostructured substrates is found to decrease the nanorod diameters. As shown in Fig. 8, when the substrate temperature was set to ~250 °C, the diameters of bundle-like ZnO nanorods decrease to about 30 nm. Therefore, these preliminary observations suggest that the ZnO nanoparticle play an important role in the formation of 1D ZnO nanorods.
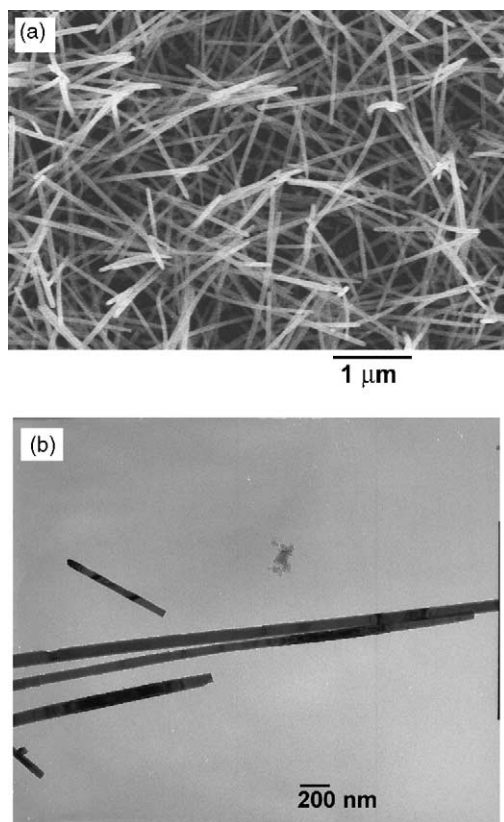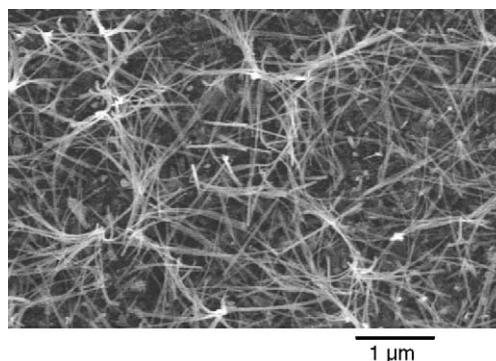

Fig. 7. (a) SEM and (b) TEM images of the ZnO nanorods grown under same condition expect using nanoparticles precursor concentration of about 0.05 M.

Based on the above observations, ZnO nanoparticles are demonstrated to have an essential effect on ZnO nanorod formation. However, in the present two-step method, the nanorods formation above nanostructured substrates cannot be explained by the well-known vapor–liquid–solid growth mechanism [11] which a liquid metal droplet is located at the growth front. As a result, a possible explanation of the crystal ZnO (c-ZnO) nanorods growth was believed to be common crystal growth by solution chemistry. For the metal-oxide growth, nucleation always needs to overcome higher activation energy barrier, and the interface energy between c-ZnO/ITO substrate is usually smaller than that of c-ZnO/solution. As a result, the nuclei will trend to create on the ITO substrate than in the solution. Moreover, the nanoparticles on substrates could further lower the c-ZnO/substrate interface energy barrier, so the nucleation of ZnO nanorods can take place in lower saturation ratio. As the hydroxyl groups on ZnO nanoparticle surface form a $ZnO/Zn(OH)_2$ core-shell nanostructure [29], electrostatic absorption (binding) could promote to the metal-organic molecule, then anchoring on the nanoparticle surfaces. Upon the hydrolysis–condensation reaction, the as-prepared ZnO nanoparticles can serve as nuclei for the directly epitaxial growth of ZnO nanorods because of the same crystal structure and lattice parameter. Compared with other reports [11–17], it should be emphasized that much lower growth temperature in our method is of particular significance and can be very helpful to complex advanced nanodevice integration where the conducting layer (such as metal) cannot survive at a high temperature.

4. Conclusions

In summary, a novel two-step procedure for preparing large-scale growth of single crystal ZnO nanorods on nanostructured substrates by soft solution method without metal catalyst is proposed. The low-temperature growth can be achieved via the help of ZnO nanostructured substrate which offers a desirable route for large-scale ZnO nanorods

growth. XRD, Raman, SEM, TEM and HRTEM analysis indicate that the diameters of single crystal ZnO nanorods with hexagonal wurtzite structure have a finite size distribution. The room temperature PL spectra of the ZnO nanorods exhibit a strong UV emission of 378 nm and a weak green emission of 580 nm. The low-temperature growth process requires no expensive and precise vacuum equipment, so permitting large-scale fabrication with a relatively low cost. In addition, the high optical transparency and electrical conductivity of the ITO glass substrates also provide a great potential in future optoelectronic nanodevice applications.

Acknowledgements

References

[1] A.M. Morales, C.M. Libber, Science 279 (1998) 208.
[2] H. Dai, E.W. Wong, Y.Z. Lu, F. Shoushan, C.M. Libber, Nature 375 (1995) 769.
[3] W.Q. Ham, S.S. Fan, Q.Q. Li, Y.D. Hu, Science 277 (1997) 1287.
[4] J.H. Zhang, X.G. Yang, D.W. Wang, S.D. Li, Y. Xie, Y.N. Xia, Y.T. Qian, Adv. Mater. 12 (2000) 1348.
[5] J.H. Hu, T.W. Odom, C.M. Libber, Acc. Chem. Res. 32 (1999) 435.
[6] X. Wang, Y. Li, J. Am. Chem. Soc. 124 (2002) 2880.
[7] L. Vayssieres, K. Keis, A. Hagfeldt, S.-E. Lindquist, Chem. Mater. 13 (2001) 4386.
[8] K. Hara, T. Horiguchi, T. Kinoshita, K. Sayama, H. Sugihara, H. Arakawa, Sol. Energy Mater. Sol. Cells 64 (2000) 115.
[9] M.H. Huang, S. Mao, H. Feick, H. Yan, Y. Wu, H. Kind, E. Weber, R. Russo, P. Yang, Science 292 (2001) 1897.
[10] M.J. Zheng, L.D. Zhang, G.H. Li, W.Z. Shen, Chem. Phys. Lett. 363 (2002) 123.
[11] M.H. Haung, Y. Wu, H. Feick, N. Tran, E. Webber, P. Yang, Adv. Mater. 13 (2001) 113.
[12] J.-J. Wu, S.-C. Liu, Adv. Mater. 14 (2002) 215.
[13] W.I. Park, D.H. Kim, S.-W. Jung, G.-G. Yi, Appl. Phys. Lett. 80 (2002) 4232.
[14] B.D. Yao, Y.F. Chan, N. Wang, Appl. Phys. Lett. 81 (2002) 757.
[15] Z.W. Pan, Z.R. Dai, Z.L. Wang, Science 291 (2001) 1947.
[16] Y.C. Kong, D.P. Yu, B. Zhang, W. Fang, S.Q. Feng, Appl. Phys. Lett. 78 (2001) 407.
[17] Y. Dai, Y. Zhang, Q.K. Li, C.W. Nan, Chem. Phys. Lett. 358 (2002) 83.
[18] L. Guo, Y.L. Ji, H. Xu, P. Simon, Z. Wu, J. Am. Chem. Soc. 124 (2002) 14864.
[19] J. Zhang, L.D. Sun, C.S. Liao, C.H. Yan, Chem. Commun. (2002) 262.
[20] O. Milosevic, D. Uskokovic, Mater. Sci. Eng. A 168 (1993) 249.
[21] L. Vassieres, K. Keis, S.-E. Lindquist, A. Hagfeldt, J. Phys. Chem. B 105 (2001) 3350.
[22] M. Haase, H. Weller, A. Henglein, J. Phys. Chem. 92 (1988) 482.
[23] U. Koch, A. Fojtik, H. Weller, A. Henglein, Chem. Phys. Lett. 122 (1985) 507.
[24] E.A. Meulenkamp, J. Phys. Chem. B 102 (1998) 5566.
[25] X.L. Xu, S.P. Lau, J.S. Chen, G.Y. Chen, B.K. Tay, J. Cryst. Growth 223 (2001) 201.
[26] J.Q. Hu, Q. Li, N.B. Wong, C.S. Lee, S.T. Lee, Chem. Mater. 14 (2002) 1216.
[27] D.M. Bagnall, Y.F. Chen, Z. Zhu, T. Yao, M.Y. Shen, T. Goto, Appl. Phys. Lett. 73 (1998) 1038.
[28] K. Vanheusden, W.L. Warren, C.H. Seager, D.R. Tallant, J.A. Voigt, B.E. Gnade, J. Appl. Phys. 79 (1996) 7983.
[29] H. Zhou, H. Alves, D.M. Hofmann, W. Kriegseis, B.K. Meyer, G. Kaczmarzyk, A. Hoffmann, Appl. Phys. Lett. 80 (2002) 210.